International Journal of Heat and Mass Transfer 87 (2015) 557–567

Contents lists available at ScienceDirect

International Journal of Heat and Mass Transfer

journal homepage: www.elsevier.com/locate/ijhmt

Heat transfer augmentation of a channel flow by active agitation and surface mounted cylindrical pin fins

Smita Agrawal [a], Terrence W. Simon [a,*], Mark North [b], Daniel Bissell [c], Tianhong Cui [a]

[a] Department of Mechanical Engineering, University of Minnesota, Minneapolis, MN 55455, USA
[b] Thermacore Inc., Lancaster, PA 17601, USA
[c] TSI Incorporated, Shoreview, MN 55126, USA

ARTICLE INFO

Article history:
Received 11 October 2014
Received in revised form 12 April 2015
Accepted 13 April 2015
Available online 29 April 2015

Keywords:
Agitation
Pin fins
Heat transfer
Electronics cooling

ABSTRACT

With the intent of enhancing heat transfer, agitation of air flow is produced inside a high-aspect-ratio rectangular channel by means of a translationally oscillating plate. So that the test simulates channel flow between fins of a heat sink for cooling of electronics, the channel is open at one end, allowing oscillatory inflow and outflow at that end. At the other end where the roots of the fins that constitute the heat sink channel walls reside, there is a gap between the moving agitator plate and the channel base. Local heat transfer rates and velocity measurements are made within different regions of the channel. Heat transfer measurements are made on a channel wall augmented with cylindrical pin fins. They compared with equivalent measurement results taken on a smooth wall channel. An increase of 4–7%, based on total wetted area is found in the heat transfer coefficient, generally, when the pin fins are introduced. The change varies according to location within the channel, however. For instance, the heat transfer coefficient in the region near the base of the fins actually decreases 4–5% (again, based on total wetted area) when the pin fins are added. In this region, the flow passing through a tip gap between the agitator tip and the channel base wall, creates strong vorticity and high near-wall shear. These features of the flow are partially blocked by the pin fins, decreasing the effectiveness of the vorticity. Important to note in these comparisons, however, is that the pin fins offer an additional 30% heat transfer area. To help explain the observed trends, velocity measurements were taken with a single-component laser Doppler anemometer in the presence of pin fins as well as in the absence of pin fins. Pin fins lead to a loss of near-wall momentum but create greater mixing and three dimensionality of the near-surface flow.

1. Introduction

Agitation can be used as an effective mixing mechanism. It can be useful where flows must be well mixed for transport of quantities within the flow or from the wall to the flow. In the present study, the flow is agitated in a representative channel of an electronics cooling heat sink heat exchanger by means of a translationally oscillating plate within the channel. The open end of each channel of the heat exchanger allows inflow and outflow of air from and to a plenum as a result of the agitator motion. The objective is to get maximum heat transfer enhancement from this arrangement. Various factors can affect the processes of heat transfer and mixing, one of them being the smoothness of the channel wall. Augmented surface features like pins can lead to enhanced near-wall mixing and increased heat transfer area. Pin fins have been used in many applications such as electronics cooling and gas turbines for enhancing heat transfer by generating vortices, free shear layers and turbulent transport.

In the present study, heat transfer and velocity measurements were done in the presence of agitation and channel wall surface augmentation with pin fins in a Large Scale Mock Up (LSMU) test facility. The LSMU facility allows resolution both in time and space for these measurements.

Agrawal [1,2] et al. carried out a detailed heat transfer and velocity field study for a similar LSMU arrangement but with plain walls. They found that agitation can lead to considerable activity inside a channel and can, therefore, cause significant heat transfer enhancement. Such an arrangement can find application in an electronics cooling heat sink. Agitation may be by an oscillating plate that mixes the flow inside a channel to augment the cooling provided by throughflow. Yeom et al. [3] did experiments to test this idea for a single channel of the heat sink at the actual scale. The channel was cooled both by agitation and throughflow.

* Corresponding author. Tel.: +1 612 625 5831.
E-mail address: simon002@umn.edu (T.W. Simon).

http://dx.doi.org/10.1016/j.ijheatmasstransfer.2015.04.036
0017-9310/

Nomenclature

f	frequency of agitator (Hz)
U_{peak}	agitator maximum speed (m/s)
Re_{peak}	Reynolds number based on agitator maximum speed
L	length scale, agitator to fin maximum distance (mm)
H	height of the channel (mm)
w	width of channel (mm)
δ_{tip}	distance between agitator tip and channel tip wall (mm)
A_a	amplitude of agitation, mean to peak (mm)
π_a	agitator width (mm)
h	heat transfer coefficient (W/m^2 K)
V	voltage (V)
I	current (A)
A	area of plate (m^2)
T_s	temperature of plate (K)
P	power supplied to copper plate (W)
$Q_{net,in}$	heat flows from neighboring copper plates (W)
T_{sink}	sink temperature (K)
U_{mean}	ensemble averaged mean velocity (m/s)
$U_i(t)$	velocity measurement at time t within the cycle number i (m/s)
U'_{RMS}	ensemble averaged RMS velocity (m/s)
Nu	Nusselt number
Str	Strouhal number
k	thermal conductivity of air (W/m K)
U_{avg}	average speed over a cycle (m/s)
Re_{flow}	Reynolds number based on averaged flow velocity in one cycle
v	kinematic viscosity of air (m^2/s)
H_p	pin fin height (mm)
D_p	pin fin diameter (mm)
S_p	spanwise spacing between pin fins (mm)

Frequencies of about 1000 Hz and amplitudes of about 1.4 mm were achieved using this technology. They were able to observe an improvement in heat transfer rate of about 55% compared to that with the non-agitated state.

Yu et al. [4] numerically studied factors influencing heat transfer for channels cooled by translationally oscillating agitators operating at the actual scale. Enhancements as high as 61% were observed. Heat transfer enhancement was found to increase with increases in amplitude or frequency. They found that heat transfer enhancement was primarily effected by the agitation velocity, the product of amplitude and frequency, with amplitude being only slightly more important than frequency. Yu et al. [5] numerically studied heat transfer enhancement obtained when heat sinks with fan-induced throughflow are assisted by active devices like agitators and synthetics jets. Their study was done for a representative single channel of a heat sink. An enhancement of about 82% was found when the performance was compared with the channel-flow-only case. In another study, Yeom et al. [6] found 91% enhancement when the channel with throughflow was assisted by agitation at a frequency of 1140 Hz, compared to a channel with throughflow only, both with 45 LPM of channel flow rate. Yeom et al. [7] reported that a thermal resistance for the heat sink of 0.053 K/W could be achieved, based on a test with a single channel with surface augmentation using pin fins when the agitator operated at a frequency of 686 Hz, an amplitude of 1.4 mm and the throughflow velocity was 7.9 m/s. The experiments were done in an actual-scale channel. They computed the resistance by extending the single-channel results to a full-scale system with a 26-channel/blade array to cool a 1.0 kW heat sink.

Various studies can be found in the literature that explore the effectiveness of surface modifications on mixing and heat transfer. Roeller et al. [8] made average heat transfer measurements and detailed flow measurements using a Laser Doppler Velocimetry (LDV) near three-dimensional protrusions in a flow channel. Their study had application to electronics cooling. They found an increase in heat transfer with an increase in protrusion height. This increase was attributed to flow acceleration in the narrower passages caused by increasing the protrusion height. An increase in heat transfer was found also in certain cases when the protrusion height was decreased. This was due to the increased three-dimensionality of the flow and increased mixing due to turbulence generated. Siw et al. [9] studied heat transfer and pressure drop characteristics with pin fins in a rectangular channel with the pins detached from one of the endwalls. The channel simulated the internal cooling passage of a gas turbine airfoil. They experimentally studied heat transfer performance by measuring heat transfer coefficients over all surfaces, including the channel walls and the pin surfaces. The pins were detached from one of the walls to promote turbulent convection and to generate separated shear layers. This led to enhanced mixing and therefore greater heat transfer. An optimal size for the gap between the pin tops and the endwall was found. This optimum condition was when the heat transfer was maximum while the pressure drop remained low.

Moores et al. [10] studied the effect of tip clearance on pin fin array heat transfer performance. The clearance was introduced between the pin tips and the surrounding shroud. They reported an increase in mean heat transfer and a drop in pressure when the clearance was between 0.5 and 1.1 times the pin diameter. They explained that the increase in heat transfer was due to the additional surface area that was exposed to the flow. This area increase enhancement was, in some cases, partially offset by a lower heat transfer efficiency per unit of fin area when the fins were added.

Ames et al. [11] experimentally investigated the flow field in a staggered array of pin fins at various Reynolds numbers by making hot wire anemometry measurements with both single and cross-wire probes. Using a commercial CFD code, they made detailed 3D calculations, learning that flow shedding near the surface of the pins leads to the generation of unsteadiness. Armstrong and Winstanley [12] conducted a review of heat transfer in staggered pin fin arrays for turbine cooling applications. The row-resolved heat transfer rates were higher for the first few rows, followed decreased values downstream, eventually reaching an asymptotic, fully-developed value. The heat transfer rates for the pin fin and endwall surfaces were of the same magnitude. Below a certain value of pin height-to-diameter ratio, the ratio did not seem to affect the heat transfer rate significantly. However, above this value, the heat transfer rate was found to increase with increasing pin height-to-diameter ratio.

Lyall et al. [13] studied heat transfer enhancement by pin fins with a height-to-diameter ratio of unity and with different spanwise spacings for cases with Reynolds numbers in the range 5000 to 30,000. Their study revealed that heat transfer enhancement over open channel flow was higher for lower Reynolds numbers and for smaller spanwise fin spacings. Also, the pin fin surface heat transfer was found to be higher than that on the channel wall. Garimella et al. [14] studied heat transfer enhancement for staggered and inline pin fin arrays with water cooling. Streamwise spacing was found to be more significant in effecting heat transfer

enhancement, compared to spanwise spacing. A staggered arrangement led to greater heat transfer enhancement. The heat transfer data correlated well with an array-based Reynolds number. Azar et al. [15] studied the effects of pin fin density on thermal resistance of a heat sink for different air velocities. The heat sink thermal resistance was found to depend on pin fin density. However, beyond a certain pin fin density, the thermal resistance changed very little by either increasing the pin fin density or increasing the velocity.

Since the present study of pin fin heat transfer performance is in the presence of oscillatory flows, a literature study for pin fins in unsteady flows is relevant. Jeng et al. [16] carried out a study to explore the effects of oscillatory flows on heat transfer in a heat sink with pin fins. They noted instability of the flow in the passages among the fins due to periodic flow rate change. Different heights of pin fins were investigated to observe the effects of bypass clearance between the shroud of the test channel and pin fins. A flow visualization study was carried out to characterize bypass over the tip. Shown was a 20–34% increase in heat transfer for a case with no bypass. With large bypass, a decrease in heat transfer was found. Thus, their study revealed that heat transfer enhancement is obtained for a no-bypass condition or for a specified bypass range. Saha et al. [17] numerically analyzed unsteady three-dimensional flow and heat transfer in a parallel plate heat exchanger with periodically mounted pin fins. The effects of varying Reynolds number and geometrical configurations were explored. Three dimensional flow behavior was observed for all geometrical configurations with the flow becoming unsteady above a Reynolds number of 180. The Thermal Performance Factor (TPF) was found to increase with flow unsteadiness. Heat transfer was found to increase with an increase in pitch up to a certain extent but then showed a decrease with further increases in pitch. The presence of cylindrical pin fins was found to make the flow unsteady, displaying multiple frequencies. The authors noted that the generated unsteadiness leads to higher heat transfer rates compared with those of steady flow.

The present study explores the effectiveness of using pin fins for heat transfer in a channel cooled by air and agitated by a translationally oscillating plate. Heat transfer and velocity measurement results are presented for different regions of the channel to quantify inertial and unsteady effects on heat transfer augmentation. As noted, little is documented in the literature on active agitation of channel flow for wall heat transfer enhancement. Most of the literature on active enhancement relates to mixing of reactants. However, the increasing ease of fabrication of micro-machines makes active enhancement increasingly more practical.

2. Experimental setup

A Large-Scale Mock-Up test facility was constructed in a fashion that made it dynamically similar to an actual-scale, single channel that could be one of an array of the channels in an electronics cooling heat exchanger [1,2]. This large scale facility was designed to allow a study of agitation effects on heat transfer alone, without any presence of continuous throughflow, as would be present in fan-driven channel flow.

A single channel of the heat sink at the actual scale might be as wide as 3–4 mm. Measurements have been done at the actual scale [7] that report enhancement obtained by using this arrangement. A channel as small as the actual scale channel does not allow sufficient space for detailed velocity and heat transfer measurements [3–7]. Thus, a single channel was scaled up and a Large-Scale Mock-Up experimental facility was built. The details of scaling are provided in Section 2.1. The experimental facility allowed measurement of both heat transfer coefficients and flow velocities at different regions within the channel that have their unique flow features. Experiments were done with plain channel walls and with channel walls augmented with pin fins.

2.1. Scaling up

Scaling up was done such that the agitator maximum speed Reynolds number was matched between the actual scale channel and the Large Scale Mock Up experiment. The maximum agitator speed is defined as:

$$U_{peak} = 2\pi A_a f \tag{1}$$

where A_a is the amplitude of the agitator, f is the frequency of agitation.

The agitator maximum speed Reynolds number is defined as:

$$Re_{peak} = \frac{U_{peak} L}{\nu} \tag{2}$$

where L is the agitator-to-fin maximum distance when the agitator is in the mean position. If the channel width is w and π_a is the agitator width, then the characteristic length used for non-dimensionalization of this Reynolds number is: $L = (w - \pi_a)/2$. Based on this non-dimensional scaling, the Large Scale Mock Up experiment setup was 39 times the size of the actual heat sink channel. The parameters for the actual-scale channel and the mock up channel are listed in Table 1. The locations of dimensions of the actual-scale and mock up channels are shown in Fig. 2b.

2.2. Apparatus

Fig. 1a shows the Large Scale Mock Up (LSMU) Unit with the agitator plate. Fig. 1b shows a schematic view of the same. The agitator plate is driven by a Scotch yoke mechanism. The agitator plate and the channel walls are made of polycarbonate sheets. Three glass windows are embedded in the top wall of the channel to allow access for the laser beams of the LDV velocity measurements. The right wall of the test section has an array of thick copper plates. The middle row of copper plates constitutes the test plates whereas the top and the bottom rows are for guard heating. Each of the copper plates has thermocouples embedded in it to measure the temperature of the plate. The plates are heated with resistance heaters glued on their backs. Thus, the plates are heated and instrumented for measuring plate average temperature and heat flux. The plate back side is insulated to assure that all the energy supplied results in heat flow to the agitated air in the test section.

Fig. 2a shows the channel in a two-dimensional view as seen from the top in the direction of the arrow "a" marked in Fig. 1b. As can be seen from Fig. 2a, the channel is divided into three sections, the entry region, the central region and the base region. The heat transfer and velocity measurements are discussed separately for these three regions. One can see from Fig. 1b that each row of copper plates has three plates, one for each of the three regions. The glass windows embedded on the top are centered on these

Table 1
Mockup and actual size parameter values.

Parameter	Mock up	Actual scale
Channel height (H)	640 mm	16.5 mm
Channel width (w)	132 mm	3.4 mm
Agitator width (π_a)	39 mm	1 mm
Amplitude (A_a)	27 mm	0.7 mm
Tip gap (δ_{tip})	19 mm	0.5 mm
Frequency (f)	0.66 Hz	1000 Hz
Agitator to fin maximum distance (L)	47 mm	1.2 mm

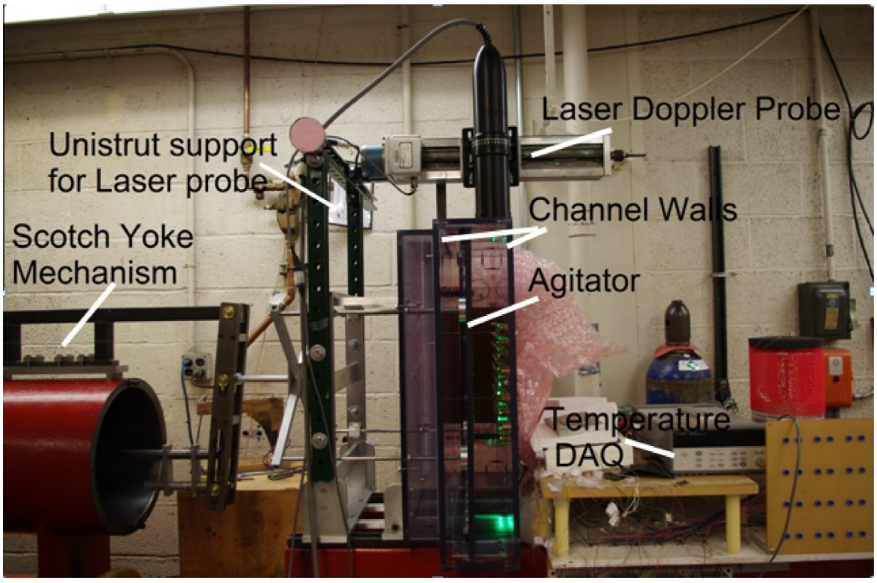

Fig. 1a. Large Scale Mock Up unit with the agitator driven by a Scotch yoke mechanism.

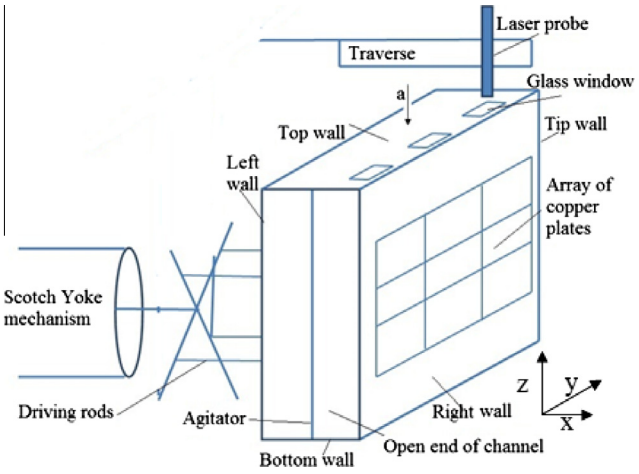

Fig. 1b. Schematic view of the mock up unit with the agitator driven by a Scotch yoke mechanism ("a" shows the view of Fig. 2a).

three regions. These glass plates allow accessibility to the laser beams for velocity measurements. As can be seen in Fig. 2a, there are three thermocouples attached to the agitator plate, each adjacent to one of these three regions, T1, T2 and T3, to measure the sink temperatures for computation of the plate-average heat transfer coefficient of each plate. The thermocouples on the agitator plate give the local flow temperature within the channel. Since, heat transfer is from the copper plates to the local air flow, the thermocouples on the agitator plate give a good convective sink temperature. The agitated air flow in the channel is well mixed. As can be seen in Fig. 2a, the agitator has a T-shaped end. This is to appropriately simulate the thickness of the agitator at the tip of the actual-scale design. In the mock up, measurements are made in the cavity on the right; thus, focus is on accurate simulation of the right side cavity.

Fig. 3 shows the staggered arrangement of pin fins on a channel wall, as fabricated for the heat transfer measurements. The arrangement of pin fins for velocity measurements is noted in Fig. 4. As can be seen in Fig. 4, a column of pins is removed for the purpose of taking velocity measurements to avoid blockage of the laser beams by pin fins. Without removing a column of pins, it would not be possible to measure velocities since the gap between consecutive columns of pins is not wide enough to allow the laser beams to pass. It was concluded that the measured velocity gave the velocity field downstream of the pin fin array regardless of flow direction. Fig. 4 shows the intersection of laser beams between pin fins for the velocity measurements.

2.3. Test section details

2.3.1. Heat transfer

The temperatures from the four thermocouples (Type E) embedded into each plate are averaged to get the average plate temperature. Their variations are less than 1 °C. The voltage difference across each heater is measured. Precision resistors with resistance of 0.2 Ω are placed in series with the power supply of each plate heater and voltage across each power resistor is measured to calculate the current to the respective heater. Experience with these heaters indicates a unity power factor; thus P = VI. An

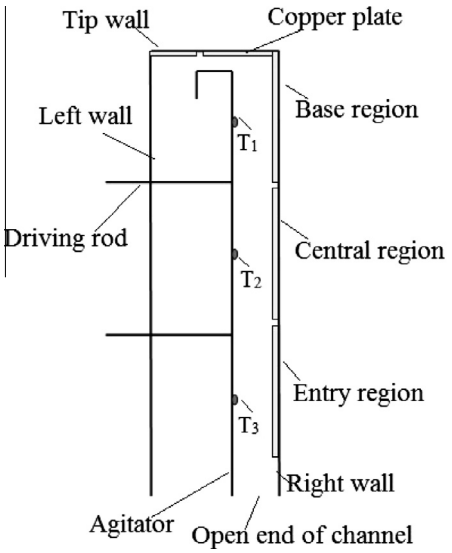

Fig. 2a. Channel in two dimensional view.

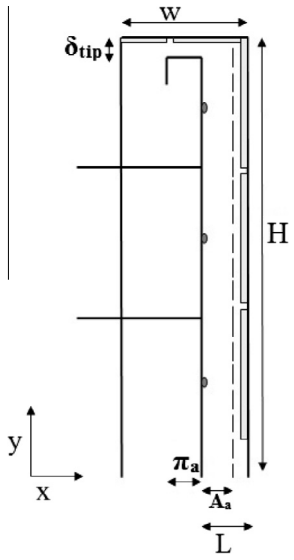

Fig. 2b. Dimensions of the channel as listed in Table 1.

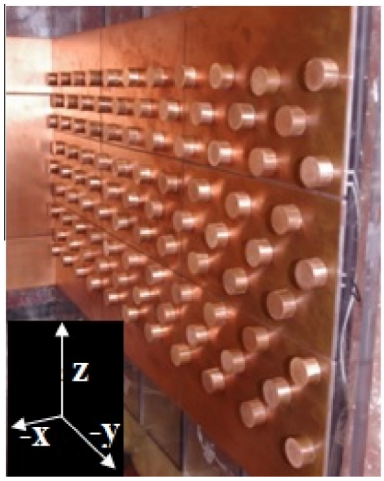

Fig. 3. Staggered arrangement of pin fins on channel wall for heat transfer measurements.

Agilent 34790A data acquisition unit (DAQ in Fig. 1a) is used to record the thermocouple voltages. The space-and-time-averaged temperatures from the thermocouples on the agitator plate are used to determine the respective heat transfer sink temperature. The heat transfer coefficient for each plate is calculated as:

$$h = \frac{VI}{A(T_s - T_{sink})} \tag{3}$$

where h is the heat transfer coefficient, V is the measured voltage, I is the current, A is the area of the heated plate segment, T_s is the plate temperature and T_{sink} is the local sink temperature. Analyses show that the plate temperature is uniform throughout its depth, so the recorded temperature is very nearly the plate surface temperature. Measurements using the same instrumentation were done when augmenting with pin fins mounted on the measurement surfaces. The pin fins, made of copper pieces, were glued on the channel wall using double-sided conductive tape. Care was taken to minimize the conductive resistance of the bond between each fin and the copper wall. The thermal resistance due to the tape junction was calculated as 0.57 K/W, which was much lower than the average convective resistance of the pin fin surface of around 60 K/W. The parameters used for the pin fins are:

$$H_p = 10\text{ mm } (0.4\text{ in}), \quad D_p = 19\text{ mm } (0.75\text{ in}), S_p = 58\text{ mm } (2.3\text{ in})$$

2.3.2. Velocity measurements

A TSI TR 60 series, two-component laser Doppler velocimetry system is used to make velocity measurements. The wall-parallel component of velocity is measured using the argon ion laser with wavelength of 514.5 nm. The laser beam diameter is 2.65 mm. For any flow measurement, velocity data are collected for approximately 80 plate oscillation cycles. The flow measurement software acquires a continuous string of data for every cycle. Data within time intervals of 0.01 s are averaged to get a representative value for that interval. As an example, data within time interval $t - 0.01$ and t are averaged to get a representative value for time t within the cycle for that particular portion of the cycle. The ensemble-averaged mean velocity at any instant, t, within the cycle is then calculated as:

$$U_{mean}(t) = \frac{1}{n}\sum_{i=1}^{i=n} U_i(t) \tag{4}$$

where i is the cycle number and t is the particular instant within the cycle. The quantity $U_i(t)$ is a velocity data point at that particular time for cycle number i.

The ensemble-averaged, RMS fluctuating velocity at cycle time t within the cycle is calculated as:

$$U'_{RMS}(t) = \left(\frac{1}{n}\sum_{i=1}^{n}(U_{mean}(t) - U_i(t))^2\right)^{1/2} \tag{5}$$

This computed velocity is non-zero due to random fluctuations of velocity from cycle to cycle. It is considered to be the measurement of turbulence level.

In the following discussion, the agitator motion is divided into four phases, as described in Fig. 5.

2.4. Uncertainty in measurements

The uncertainties associated with measurements of heat transfer coefficients, h, were calculated using the equation:

$$\delta h = \left[\left(\frac{\partial h}{\partial P}\delta P\right)^2 + \left(\frac{\partial h}{\partial Q_{net.in}}\delta Q_{net.in}\right)^2 + \left(\frac{\partial h}{\partial T_{sink}}\delta T_{sink}\right)^2 + \left(\frac{\partial h}{\partial T_s}\delta T_s\right)^2 + \left(\frac{\partial h}{\partial A}\delta A\right)^2\right]^{1/2} \tag{6}$$

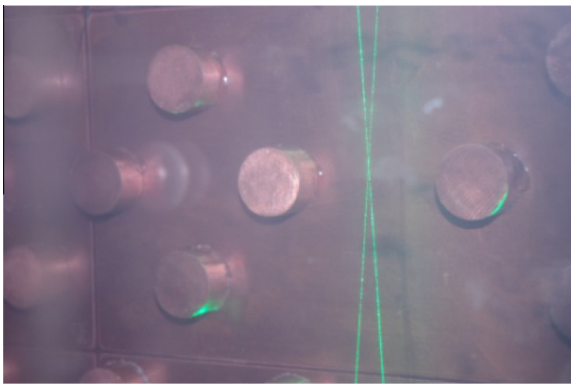

Fig. 4. Laser beams intersecting in between the pin fins for velocity measurements.

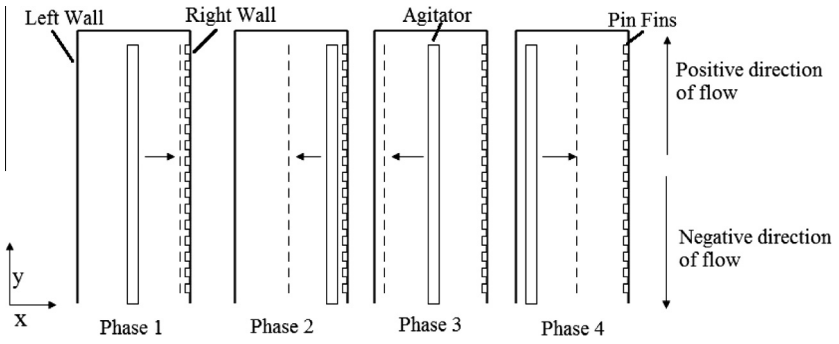

Fig. 5. Four phases of agitator motion.

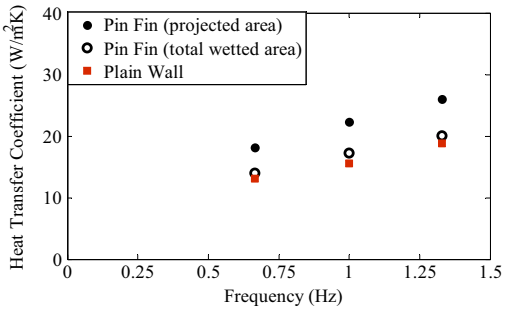

(a) Entry Region

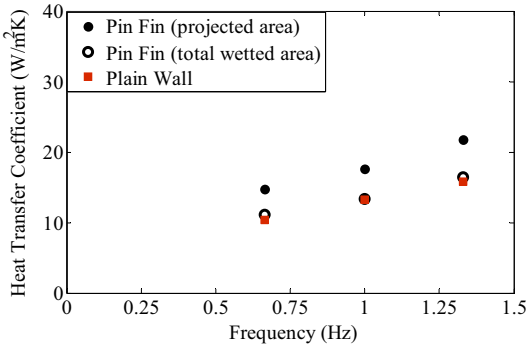

(b) Central Region

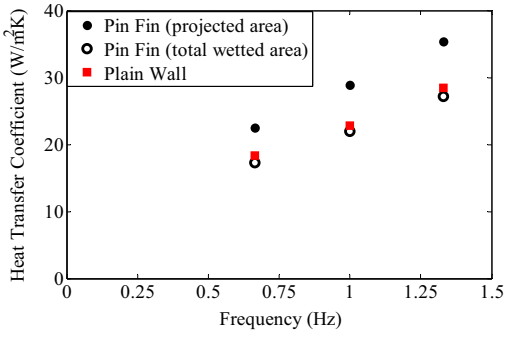

(c) Base Region

Fig. 6. Heat transfer coefficient vs. frequency for the channel with a plain wall and a channel augmented with pin fins, noted also is the effect of agitation plate oscillation frequency (mean to peak oscillation amplitude is 27 mm).

The uncertainty components are: temperature, 0.3 K; voltage, 2% of reading, plus 2 counts; precision resistor, 1% of specified resistance of 0.2 Ω. The largest term of Eq. (6)is the power uncertainty. The uncertainty associated with area is small and can be neglected in comparison to the uncertainty produced by measurement of temperature and voltage. The uncertainty associated with each measured heat transfer coefficient ranges over 6–13%. Experience with repeated runs shows repeatability to well within this interval.

The uncertainty associated with velocity measurements using the LDV system is around 0.5% of the measured velocity. Thus, accurate measurements of velocities can be reported. However, it should be noted that large spatial variations of these values are present so the particular measurements reported can be used for general discussions of flow fields representative of various regions of the flow.

3. Results and discussions

3.1. Heat transfer results

Fig. 6(a) shows the change of heat transfer coefficient on the pin fin surface with changes in frequency for the entry region (shown in Fig. 2a). The oscillation amplitude for the results discussed is 27 mm (mean-to-peak). Heat transfer coefficients increase with increasing frequency. As can be seen from Fig. 6(a), heat transfer coefficients computed in the presence of pin fins based on the projected view are about 30–40% higher when compared with plain-wall heat transfer coefficients. The projected view in this case is looking in the direction perpendicular to the pin fins' flat tip and base surfaces. Thus, when the projected view is taken, the total heat transfer area is equivalent to that of the plain flat wall. The heat transfer coefficients were calculated based on the projected view to get a sense of total enhancement in heat transfer when compared to that on the plain wall. When the heat transfer coefficient is calculated based on the wetted area, one can note about 6–7% enhancement in heat transfer coefficient for the pin fin surface. The increase in area due to the addition of pin fins is 30%.

Fig. 6(b) shows the heat transfer coefficient change with frequency in the presence of pin fins for the central region. For an oscillation amplitude (mean-to-peak) of 27 mm, about 35% enhancement can be observed due to the addition of pin fins when the heat transfer coefficient is calculated based on the projected view. When the heat transfer coefficient is calculated based on the total wetted area, a 3–4% enhancement is observed.

Fig. 6(c) shows the heat transfer coefficient change with various frequencies for the base region. When the heat transfer coefficient is computed based on the projected view, an increase of about 25% can be observed. However, when the heat transfer coefficient is calculated based on the actual wetted area, a decrease of about 4–5% can be observed for the pin fin surface.

Velocity measurements presented in the following section help to explain these observed heat transfer trends.

3.2. Velocity results

Mean velocity measurements and RMS fluctuating velocity measurements resolved in time are presented for each of the three regions in this section. Comparisons are made of velocity measurements for the case of a plain wall and for a channel wall augmented with pin fins. The pin fin height is about 10 mm. Measurements are presented for two wall-normal distances, 8 and 14 mm. Measurements at a wall normal distance of 8 mm are representative of the activity inside the pin fin array and those at a wall-normal distance of 14 mm indicate the velocity variations outside the pin fin array. The velocity measurements have been resolved according to the four phases discussed in Fig. 5 (note also the fluid velocity directions).

Fig. 7a shows the ensemble-averaged mean velocity plots for the entry region with a frequency of 0.66 Hz and amplitude of 27 mm (mean-to-peak). The plot shows the ensemble-averaged mean velocity at two wall-normal distances, 8 and 14 mm. When the mean velocity profiles are compared at a wall-normal distance of 8 mm for a plain wall and for the pin fin wall cases, one can see that the pin fin wall cases experience momentum loss. The pin fin height is 10 mm, so a wall normal-distance of 8 mm is just 2 mm below the pin fin tops. At a wall-normal distance of 14 mm (outside the pin fin array), less momentum loss is experienced in the case with pin fins when compared to that at a wall-normal distance of 8 mm. As can be seen from the plot, the variation in velocity with wall-normal distance is more when pin fins are added to the channel wall. This is an indication that even though there is momentum loss in the presence of pin fins, pin fins lead to flow mixing by causing more point-to-point variation in velocity than in the plain wall case.

Fig. 7b shows a fluctuation velocity comparison for the pin fin and plain wall cases in the entry region for a frequency of 0.66 Hz and an amplitude of 27 mm. The pin fin case shows higher velocity fluctuations than seen in the plain wall case, in general. The heat transfer coefficient results in Section 3.1 show that when the heat transfer coefficient is calculated based on the wetted area, an increase over the plain wall case of about 6–7% is observed for the pin fin wall case. This is attributed to increased turbulence and three dimensionality of the flow in the presence of pin fins.

Fig. 8a shows the ensemble-averaged mean velocity variations for the central region with a frequency of 0.66 Hz and amplitude of 27 mm, both for the plain wall case and with pin fins. The central region data are influenced by the entry region and base region flow characteristics. During phase 2, the presence of pin fins accelerates the change in the flow direction from negative to positive, when compared to flow in the plain wall case. During phase 3, the core flow outside the pin fin array (wall normal distance of 14 mm) shows increased velocities compared to those in the plain wall case, but the flow inside the pin fin array (wall normal distance of 8 mm) shows a loss of momentum, compared to that of the plain wall case. In the presence of pin fins, there is more variation in velocity from point to point, increasing the three-dimensionality of the flow. One can see higher magnitudes of mean velocity during phases 3 and 4 for the pin fin case, which leads to higher heat transfer coefficients in the central region compared to the plain wall case.

Fig. 8b shows the variation of ensemble-averaged RMS fluctuating velocity for the central region at a frequency of 0.66 Hz and amplitude of 27 mm. During phase 2, one can see a rise in fluctuating velocity at a wall-normal distance of 14 mm for the pin fin case. The slight increase in heat transfer coefficient (3–4%) mentioned in Section 3.1 can also be attributed to the slight increases in fluctuating velocity in the presence of pin fins during phases 2 and 4, as seen in Fig. 8b.

Fig. 9a shows the base region variation of ensemble-averaged mean velocity for the pin fin case and for the plain wall case at a frequency of 0.66 Hz and amplitude of 27 mm. In the presence of pin fins, as the agitator moves toward the right wall (phase 1), flow outside the pin fin array has accelerated and escapes through the tip gap region (refer to Fig. 5 for directions), but the flow inside the pin fin forest shows a delayed response to the agitator motion, taking time to accelerate. During phase 2, when the agitator moves from the right channel wall toward the center of the channel, flow is drawn into the right side channel cavity through the narrow tip gap. This drawing in of flow creates vorticity in the base region. In the plain wall case, the drawing in of flow was stronger closer to the wall, as can be seen by comparing the velocity profiles for wall-normal distances 8 and 14 mm. However, in the presence of pin fins, the overall activity of drawing in fluid has weakened significantly in the base region, with the weakening being more within the pin fin forest. It appears that the presence of pin fins causes blockage of the flow in the base region leading to reduction in velocity magnitudes. Vortical activity that would otherwise be seen in the plain wall case due to the narrow gap between the agitator tip and the channel base is reduced in the presence of pin fins in the base region.

Fig. 9b shows fluctuating velocity characteristics for the base region for a frequency of 0.66 Hz and amplitude of 27 mm. During phase 1, the fluctuation magnitude of velocity is higher for the pin fin case within the pin fin array (wall-normal distance 8 mm) than outside the pin fin array (wall-normal distance 14 mm). Thereafter, for all other phases, it can be noted that the fluctuation velocity magnitude in the presence of pin fins is lower than when they are absent. This could be attributed to blockage provided by the pin fins in the base region and significantly reduced mean velocities due to pin fins during phases 2, 3 and 4. In the base region, both the mean velocities and fluctuating velocities are lower than those of the plain wall case. Thus, base region heat transfer coefficients computed using the total wetted area show a decrease of about 5% in the presence of pin fins.

3.3. Non-dimensional heat transfer results

The heat transfer and velocity results presented in Sections 3.1 and 3.2 have been non-dimensionalized to further explain the role of inertial effects and unsteady effects in augmenting heat transfer. This flow has agitation; thus, along with inertial and turbulence effects, we have unsteady effects that play a role in enhancing heat transfer.

The length scale used for non-dimensionalizing is the agitator-plate-to-channel-wall maximum distance when the agitator is in its mean position. Thus, the Nusselt number is calculated as:

$$Nu = \frac{hL}{k} \tag{7}$$

where h is the measured heat transfer coefficient as shown in Fig. 6(a)–(c) and k is the thermal conductivity of air.

The characteristic velocity, U_{avg}, is the average speed over a cycle in the free stream zone for each region (U_{avg} is calculated by averaging the speed over a cycle, measured at a wall-normal distance of 14 mm, which is considered to be in the free stream zone). The Strouhal number is calculated as:

$$Str = \frac{fL}{U_{avg}} \tag{8}$$

where f is the agitator oscillation frequency. The Reynolds number is calculated as:

$$Re_{flow} = \frac{U_{avg}L}{\nu} \tag{9}$$

where ν is the kinematic viscosity of air.

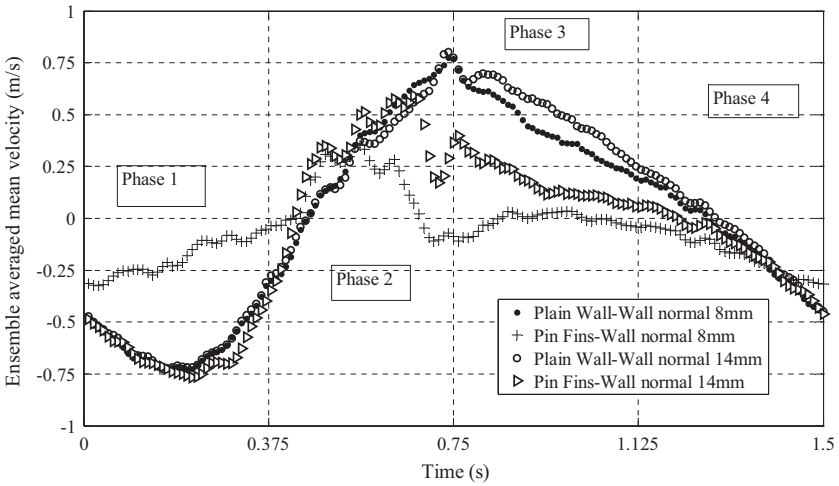

Fig. 7a. Entry region, ensemble-averaged mean velocity comparison for plain wall vs. pin fin walls for frequency 0.66 Hz and amplitude 27 mm.

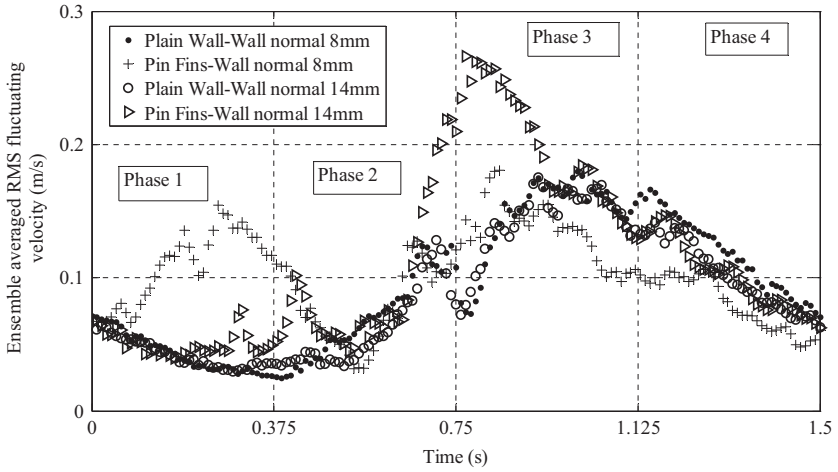

Fig. 7b. Entry region, ensemble-averaged RMS fluctuating velocity comparison for plain wall vs. pin fin walls for frequency 0.66 Hz and amplitude 27 mm.

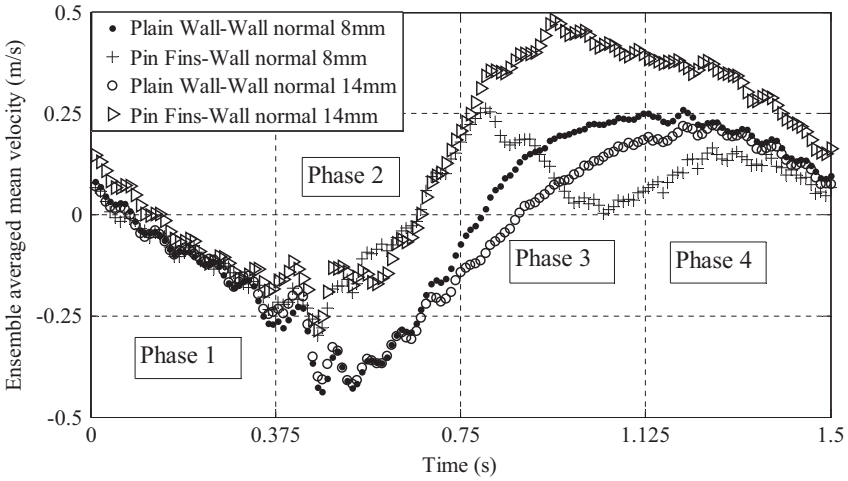

Fig. 8a. Central region, ensemble-averaged mean velocity comparison for plain wall vs. pin fin walls for frequency 0.66 Hz and amplitude 27 mm.

The Nusselt number variation vs. Reynolds number is shown in Fig. 10(a)–(c), both for the pin fin case and the plain wall case for each of the three regions. The Strouhal number has a different value for each region and each wall geometry but does not vary much with Reynolds number except for the central region for the plain wall configuration. For central region, for plain wall, the

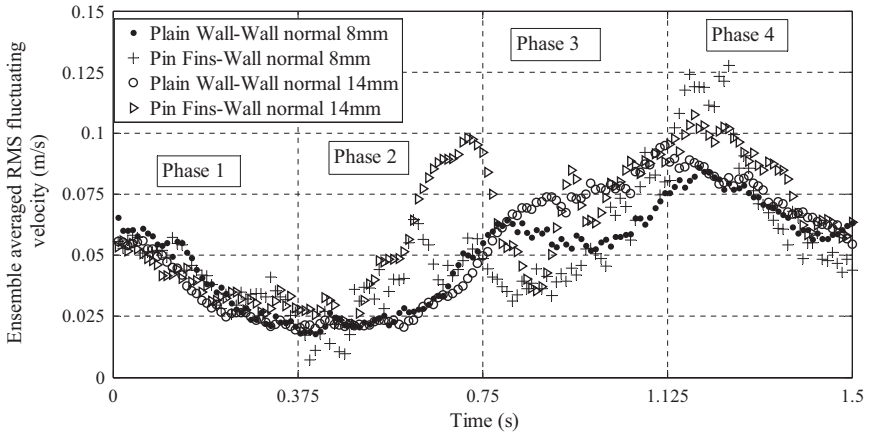

Fig. 8b. Central region, ensemble-averaged RMS fluctuating velocity comparison for plain wall vs. pin fin walls for frequency 0.66 Hz and amplitude 27 mm.

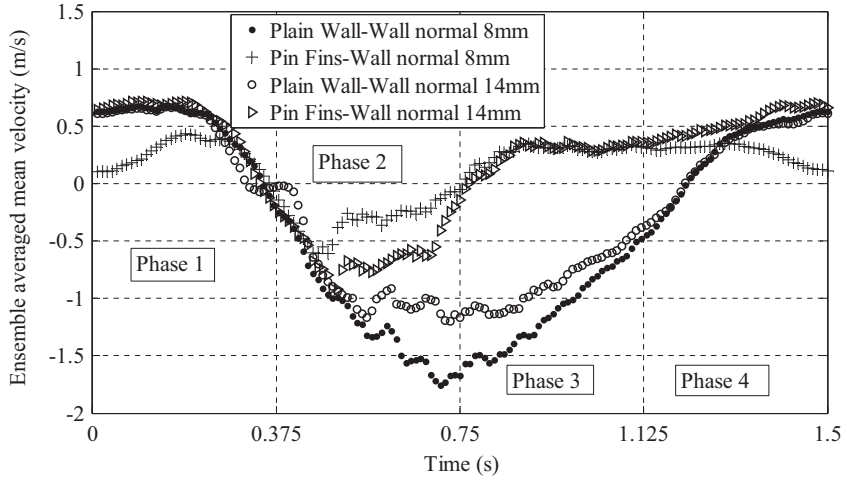

Fig. 9a. Base region, ensemble-averaged mean velocity comparison for plain wall vs. pin fin walls for frequency 0.66 Hz and amplitude 27 mm.

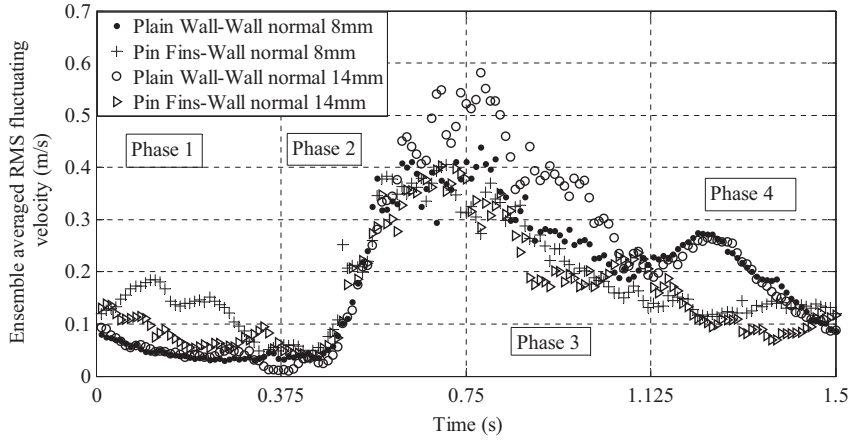

Fig. 9b. Base region, ensemble-averaged RMS fluctuating velocity comparison for plain wall vs. pin fin walls for frequency 0.66 Hz and amplitude 27 mm.

Strouhal number has a value of 0.19 at a Reynolds number of 488 and a value of 0.21 at Reynolds number 672 and 883. So, for a particular region, if the wall geometry (smooth/plain) does not change, the Strouhal number does not change much. This is because the measured velocities scale with agitation frequency. There seem to be two effects enhancing heat transfer, inertial effects, indicated by Reynolds number, and unsteady effects, indicated by Strouhal number.

For the plain wall case, the Reynolds number is high in the base region, with reduced values in the entry region and even lower values in the central region. The Strouhal number is high in the central region followed by the entry region and base region. The

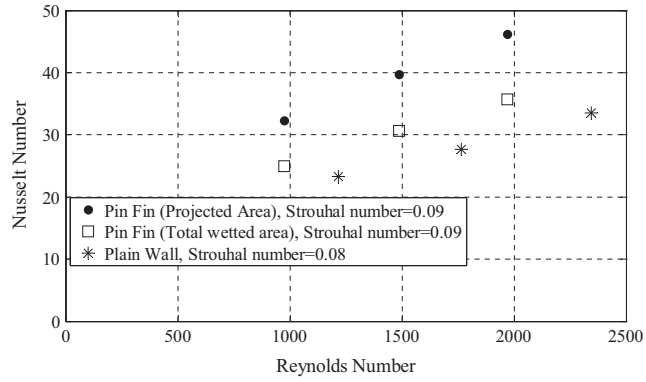

(a) Entry Region

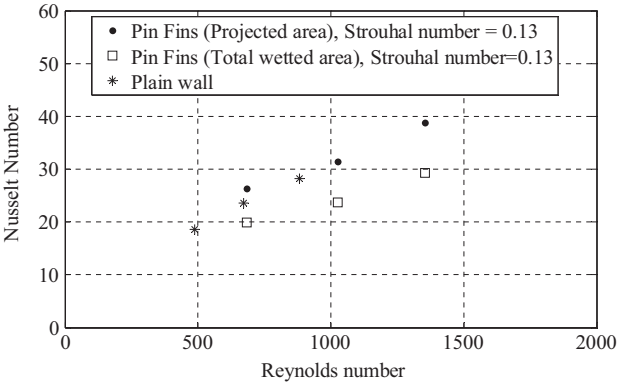

(b) Central Region

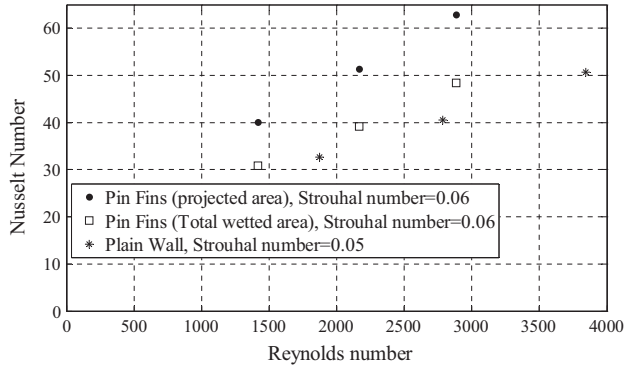

(c) Base Region

Fig. 10. Variation of Nusselt number with Reynolds number for the three regions.

data show unsteady effects are more dominant in the central region for the plain wall case. For the entry and base regions, the Strouhal number is higher for the pin fin case than for the plain wall case. Thus, for the entry and base regions, unsteadiness may be more important than inertial effects in enhancing heat transfer coefficients for the pin fin case. For the central region, Strouhal number is higher for the plain wall case than for the pin fin case. Thus, for central region unsteady effects are more dominant for the plain wall case.

This analysis helps us in understanding the mechanism of heat transfer enhancement for each of the three regions both for the plain wall configuration and for the pin fin configuration. For design purposes, it lends insight into the relative importance of Reynolds number and Strouhal number in influencing heat transfer enhancement for a particular region and wall characteristic.

4. Conclusions

Heat transfer and velocity measurements have been made in a rectangular channel with an oscillating plate called the agitator. The agitator generates mixing within the flow and leads to convective heat transfer enhancement. With agitation, flow and heat transfer comparisons are made between a case with pin fins on the channel wall and another with a plain wall.

Pin fins lead to a loss of momentum but generate additional turbulence. Addition of pin fins leads to greater mixing and three-dimensionality of the flow in the entry region (the region nearest the plenum of the heat sink channel). An increase of about 6–7% is found in the entry region based on the total wetted area when the heat transfer coefficient is compared with that of the plain wall case.

An increase of about 3–4% in heat transfer coefficient is found in the central region in the presence of pin fins when the total wetted area is taken into account. This is attributed to greater mean velocity in the presence of pin fins in the central region.

A decrease in heat transfer coefficient based on wetted area of about 5% is found in the base region (the region nearest the base of the channel) when pin fins are added. This decrease is attributed to flow blockage experienced in the base region in the presence of pin fins. Both mean velocities and fluctuating velocities show reductions in magnitude in the presence of pin fins in the base region.

The heat transfer results have been non-dimensionalized to separate the unsteady and inertial effects in augmenting heat transfer. When comparison is made between the plain wall case and the pin fin case for entry and base regions, inertial effects are found to be more important than unsteady effects in influencing heat transfer for the plain wall case. For the central region, since the velocities are higher for the pin fin case, inertial effects seem to be more important in the pin fin case than in the plain wall case. In the central region of the plain wall case where the flow might be characterized as an unsteady boundary layer flow, unsteadiness seems to be the dominant factor.

These results help us understand the conditions under which turbulence and unsteadiness effects may be more important for effecting wall heat transfer enhancement in agitated channel flow. The three regions of the channel have different flow characteristics. The entry region has an unsteadily driven channel flow activity. The base region has vortical activity. The central region is influenced by the activities in the entry and the base region. This study provides details of agitation for different flow characteristics and the influence of agitation on heat transfer in the presence of smooth walls and surfaces augmented with pin fins. It has applications in electronics cooling [3–7] and other fields where heat transfer enhancement is desirable by agitation. The detailed understanding lends insights into the mechanism of heat transfer, which further assists in better design of heat sinks and agitators to get maximum heat transfer benefit.

Conflict of interest

None declared.

Acknowledgments

This work was supported in part by the Defense Advanced Research Projects Agency (DARPA) MACE Program. The views expressed are those of the authors and do not reflect the official policy or position of the Department of Defense or the US Government. Approved for Public Release, Distribution Unlimited.

References

[1] S. Agrawal, T. Simon, M. North, T. Cui, An experimental study on the effects of agitation on forced-convection heat transfer, in: Proceedings of ASME 2011 International Mechanical Engineering Congress and Exposition, Denver, Colorado, IMECE 2011-64558, 2011, pp. 905–912,.

[2] S. Agrawal, T. Simon, M. North, T. Cui, An experimental study on the effects of agitation in generating flow unsteadiness and enhancing convective heat transfer, in: Proceedings of ASME 2012 Summer Heat Transfer Conference, Puerto Rico, HT 2012-58273, pp. 649–657.

[3] T. Yeom, T.W. Simon, L. Huang, M. North, T. Cui, Piezoelectric translational agitation for enhancing forced-convection channel-flow heat transfer, Int. J. Heat Mass Transfer 55 (2012) 7398–7409.

[4] Y. Yu, T.W. Simon, T. Cui, A parametric study of heat transfer in an air-cooled heat sink enhanced by actuated plates, Int. J. Heat Mass Transfer 64 (2013) 792–801.

[5] Y. Yu, T.W. Simon, M. Zhang, T. Yeom, M. North, T. Cui, Enhancing heat transfer in air cooled heat sinks using piezoelectrically-driven agitators and synthetic jets, Int. J. Heat Mass Transfer 68 (2014) 184–193.

[6] T. Yeom, T.W. Simon, Y. Yu, M. North, T. Cui, Convective heat transfer enhancement on a channel wall with a high frequency, oscillating agitator, in: Proceedings of ASME 2011 International Mechanical Engineering Congress and Exposition, IMECE 2011-64379, Denver, USA, 2011, pp. 875–884.

[7] T. Yeom, T.W. Simon, Y. Yu, M. Zhang, S. Agrawal, L. Huang, T. Zhang, M. North. T. Cui, An active heat sink system with piezoelectric translational agitators and micro pin fin arrays, in: Proceedings of ASME 2012 International Mechanical Engineering Congress and Exposition, IMECE 2012-88449, Houston, Texas, 2012, pp. 1479–1488.

[8] P.T. Roeller, J. Stevens, B.W. Webb, Heat transfer and turbulent flow characteristics of isolated three-dimensional protrusions in channels, J. Heat Transfer 113 (3) (1991) 597–603.

[9] S.C. Siw, M.K. Chyu, T.I.-P. Shih, M.A. Alvin, Effects of pin detached space on heat transfer and pin fin arrays, J. Heat Transfer 134 (2012) 081902-1–081902-9.

[10] K.A. Moores, Y.K. Joshi, Effect of tip clearance on the thermal and hydrodynamic performance of a shrouded pin fin array, J. Heat Transfer 125 (6) (2003) 999–1006.

[11] F.E. Ames, L.A. Dvorak, Turbulent transport in pin fin arrays: experimental data and predictions, J. Turbomach. 128 (1) (2005) 71–81.

[12] J. Armstrong, D. Winstanley, A review of staggered array pin fin heat transfer for turbine cooling applications, J. Turbomach. 110 (1) (1988) 94–103.

[13] M.E. Lyall, A.A. Thrift, K.A. Thole, A. Kohli, Heat transfer from low aspect ratio pin fins, J. Turbomach. 133 (1) (2011) 011001-1–011001-10.

[14] S.V. Garimella, P.A. Eibeck, Heat transfer characteristics of an array of protruding elements in single phase forced convection, Int. J. Heat Mass Transfer 33 (12) (1990) 2659–2669.

[15] K. Azar, C.D. Mandrone, Effect of pin fin density of the thermal performance of unshrouded pin fin heat sinks, J. Electron. Packag. 116 (4) (1994) 306–309.

[16] T.M. Jeng, S.C. Tzeng, W.T. Hsu, G.W. Xu, Flow visualization and heat transfer characteristics of oscillating fluid through pin-fin array in a rectangular channel, Adv. Mech. Eng. 2013 (2013) 1–7. Article Id 283830.

[17] A.K. Saha, S. Acharya, Parametric study of unsteady flow and heat transfer in a pin-fin heat exchanger, Int. J. Heat Mass Transfer 46 (20) (2003) 3815–3830. Journal Paper.